

Article

Analysis of NDVI Trends and Driving Factors in the Buffer Zone of the Aral Sea

Mengqi Cui ^{1,2,3}, Xinjun Zheng ^{1,2,*}, Yan Li ^{2,4} and Yugang Wang ^{1,2}

¹ State Key Laboratory of Desert and Oasis Ecology, Xinjiang Institute of Ecology and Geography, Chinese Academy of Sciences, Urumqi 830011, China; cuimengqi18@mailsucas.ac.cn (M.C.); wangyg@ms.xjb.ac.cn (Y.W.)

² Fukang Station of Desert Ecology, Chinese Academy of Sciences, Fukang 831505, China; liyan@ms.xjb.ac.cn

³ University of Chinese Academy of Sciences, Beijing 100049, China

⁴ State Key Laboratory of Subtropical Silviculture, Zhejiang A&F University, Hangzhou 311300, China

* Correspondence: zhengxj@ms.xjb.ac.cn

Abstract: A buffer zone can be used to analyze the influence of the lake on the surrounding spatial elements, which is of great significance for discussing the problems of lake retreat, vegetation degradation, and overall environmental deterioration in the Aral Sea. Taking the 3 km buffer zone of the Aral Sea as the research area, the spatiotemporal variation characteristics and main influencing factors of the Normalized Difference Vegetation Index (NDVI) in the Aral Sea research area were studied using remote sensing over 31 years (1987, 1997, 1992, 2007, 2010, 2014, 2015, 2017, and 2018). The results showed that the vegetation growth in the Aral Sea buffer zone deteriorates with the retreat of the lake; the vegetation of the small Aral Sea began to recover due to the stable water volume and salt content of the lake; vegetation began to grow in the west coast of the West Aral Sea; the shrinkage of the Aral Sea caused by human activities is an important factor affecting the growth of the vegetation. This study provides a reference for the restoration and reconstruction of regional vegetation.

Keywords: buffer zone; NDVI; lake; the Aral Sea; vegetation



Citation: Cui, M.; Zheng, X.; Li, Y.; Wang, Y. Analysis of NDVI Trends and Driving Factors in the Buffer Zone of the Aral Sea. *Water* **2023**, *15*, 2473. <https://doi.org/10.3390/w15132473>

Academic Editors: Junhong Bai, Tian Xie, Laibin Huang and Christos S. Akrotos

Received: 19 April 2023

Revised: 30 June 2023

Accepted: 3 July 2023

Published: 5 July 2023



Copyright: © 2023 by the authors. Licensee MDPI, Basel, Switzerland. This article is an open access article distributed under the terms and conditions of the Creative Commons Attribution (CC BY) license (<https://creativecommons.org/licenses/by/4.0/>).

1. Introduction

Lakes are important ecosystems providing various ecosystem services [1]. They provide habitat for a wide range of species and form essential components in hydrological, nutrient, and carbon cycles [2,3]. In arid areas with fragile ecosystems, lakes regulate climate [4], support ecological functions [5], and support human populations. Vegetation plays an important role in regulating terrestrial carbon balance and improving local environments [6–8]. Monitoring vegetation dynamic changes has important scientific significance and practical value [9]. A lake buffer zone generally refers to some land areas above the highest water level of lakes, reservoirs, and other water bodies, and its scope varies according to the actual situation of different water bodies [10,11]. The buffer zone is an important part of the ecosystem of a lake, and it is a crucial protective barrier for lake safety [12]. This quantitative study on the characteristics of lakeside vegetation can help us understand the range and intensity of the impact of lakes on lakeside vegetation and contribute to the knowledge useful for the restoration and reconstruction of vegetation.

Since the 1960s, contemporary long-time satellite remote sensing data have been widely used in vegetation monitoring and evaluation [13,14], providing a way to monitor the surface vegetation dynamics at different spatiotemporal scales [15,16]. Remote sensing data can be used to obtain a variety of vegetation indices, reveal the spatial pattern and heterogeneity of surface vegetation growth, and meet the needs of global and regional research. With the merits of long continuous time series, good data availability of products based on different remote sensors, and indicators of photosynthetic capacity [17], the Normalized Difference Vegetation Index (NDVI) is widely used to evaluate the growth

and development of vegetation. It is an effective index to reflect the large-scale vegetation coverage and growth [7–9]. NDVI has various uses, including biomass estimation [18], plant productivity monitoring [19], plant stress detection [20], and leaf water potential estimation [21]. Nik et al. [22] created an NDVI time series extending to the contrasting dynamics of littoral and riparian reed stands within a wetland complex of Lake Cerknica. Li et al. [23] use the NDVI time series to find the monotonic trend of vegetation in China. Meng et al. [24] found the variation trends of NDVI in the Tibetan Plateau. NDVI values tend to increase as the plants develop, and NDVI time series data may, therefore, also be used for the monitoring of plant phenology [25–27]. Among the environmental impact factors, the change in NDVI can not only reflect changes in vegetation coverage but also reflect the local environmental conditions to some extent, which is of great significance to understand the ecological status of an area [28–30]. In arid areas, the environment is particularly fragile and the response of vegetation productivity is sensitive to lake retreat. Revealing the impacts of lake retreat on littoral vegetation productivity is of great significance for further understanding the characteristics of lake ecosystem change, the driving factors and response mechanisms of vegetation change, and the restoration of vegetation [31–33].

The Aral Sea is an inland lake in the arid region of Central Asia and was once the fourth-largest lake in the world [34,35]. However, due to climate change in recent decades and water resources in the lake watershed by humans, the amount of water in the lake in the Aral Sea has decreased sharply, the area has been shrinking, and the salinity has increased. This has serious negative impacts on water resources and the local ecology, causing a series of problems [36,37]. After the large-scale retreat of the Aral Sea, studying how the lakeside vegetation changes is important for ecological restoration. The present paper introduces the ecological environment crisis of the Aral Sea from the perspective of water volume, area, soil, land use, and salt dust in the area that emerged due to the retreating lake [38–41]. It focuses on the vegetation change and reconstruction in the whole Aral Sea basin and the retreat area [42–44]. The lake buffer zone is an important part of the lake ecosystem and a vital protective barrier. It is of great significance for ecological restoration.

This study analyzed the spatiotemporal vegetation dynamics and their response to environmental change in the buffer of the Aral Sea from 1987 to 2018. This paper focused mainly on the vegetation growing season (May to October). Analysis for spring (April to May), summer (June to August), and autumn (September to October) were also conducted to achieve a better understanding of seasonal changes in NDVI and their responses to environmental variation. We aimed (1) to investigate the NDVI of the buffer region inter-annual growing season during the past 30 years and explore facts and reasons for the NDVI trends; (2) to understand the range and intensity of the influence of the lake on vegetation on the lakeside; (3) distinguish potential drivers of NDVI changes, including the lake level and the lake area in the buffer region. The findings of this study serve as a fundamental knowledge base for projecting future vegetation growth trends, environmental changes, and ecosystem evolution in the buffer zone of the Aral Sea, all of which are necessary to assess the ecological security of the Aral Sea.

2. Materials and Methods

2.1. Study Area and Vegetation Inventory Data

The Aral Sea is an inland lake located on the territory of Kazakhstan and Uzbekistan in Central Asia (Figure 1), with a maximum length of 428 km from north to south, a width of 235 km from east to west, and a maximum area of 66,900 km² (including 313 islands, covering an area of 23,345 km²) [45]. This region has a continental dry climate because it is located far from the ocean. Summer temperature reaches 40 °C degrees while the temperature in winter falls below −20 °C. The mean annual precipitation is 100–250 mm, and the average monthly precipitation ranges from 6 mm (in September) to 15 mm (in March) [46,47]. It used to be the world's fourth-largest lake but has shrunk over the past few decades [48]. The water supply for the Aral Sea is dependent on the Amu Darya

and Syr Darya Rivers, which are the two major tributaries of the Aral Sea Basin [37,49–51]. These two rivers originate from the Pamirs and Tian Shan Mountains and run through the territory of Central Asia and Afghanistan [52,53]. The Amu Darya is 2540 km long and it is geographically located in the south of the Aral Sea basin, with a coverage of the catchment area of more than $30.9 \times 10^4 \text{ km}^2$ [54–56]. The Syr Darya is approximately 3000 km, the longest river in Central Asia, and ranks second in terms of water runoff [57,58]. In the 1940s, construction began on a large scale in the Aral basin, and most of them were used for agriculture. Many sections of the channel were of poor quality, causing large amounts of water to evaporate or leak [37]. The Qaraqum, Central Asia's largest aqueduct, is estimated to be only 30 to 70% water efficient. The canals around the Aral Sea's two main sources of water are also leaking, with about 20 to 60 km³ of water diverted from the Amu Darya and Syr Darya rivers to the desert every year [45]. Since the 1960s, human's high-intensity utilization of water and soil resources has led to the long-term over-exploitation of water resources in the Amu Darya and Syr Darya Rivers [59,60], and the Aral Sea has experienced a sharp reduction in water (Figure 2a,b), which has produced serious negative effects on water resources and the local ecology. The Soviet Union vigorously expanded agriculture, especially cotton cultivation, from about 4.5 million ha in 1960 to nearly 7 million ha in 1980 [35]. The local population has grown rapidly, from 14 million to about 27 million over the same period, and the total water intake has almost doubled [56]. At the same time, the destruction of the water balance in the Aral Sea basin, the overexploitation of many small tributaries, and the inefficiency of irrigation have contributed to massive waterlogging and salinity [61]. By 1990, more than 95 percent of the marshes and wetlands had become deserts, and more than 50 percent of the Delta's lakes had dried. Salty dust is blown from the exposed lake bed to nearby farmland, degrading the soil and forcing crops to draw more river water to sustain their growth, creating a vicious cycle [61–63]. This phenomenon grabbed worldwide attention in the 1990s and has since been dubbed “the Aral Sea crisis” [36,37]. In 1986, the main body of the Aral Sea split into two parts—the Large Aral Sea (the South Aral Sea) and the Small Aral Sea (the North Aral Sea). In 2003, Kazakhstan built the Kok-Aral Dam between the Large Aral Sea and the Small Aral Sea to improve the environment around the Small Aral Sea and prevent water from flowing to the Large Aral Sea [64]. In 2005, the completion of the Kok-Aral Dam blocked the Syr River's flow into the Large Aral Sea. Since then, the shrinking of the Small Aral Sea has slowed down [65]. In recent years, the water volume has increased (Figure 2a), and the salinity of the lake has begun to decline [66] (Figure 2c). In 2007, the Large Aral Sea split into two parts: the East Aral Sea and the West Aral Sea [51].

In 2019, we conducted a survey and sampling of the Aral Sea. The Aral Sea is located in the temperate zone hungeriness take of Central Asia. In the western plateau area, the desert vegetation species are relatively simple, and the coverage is relatively uniform but low; the main plant types are *Artemisia* and *Ephedra* and other dwarf semi-shrubs, about 20 cm in height; there are ephemerals, such as Gramineae, with low density. The east island is high in terrain and well-covered by vegetation, mainly composed of salt-tolerant desert plants such as *Haloxylon ammodendron*. From Nukus to Tashkent, the desert plants are mainly clustered in *Artemisia*, Chenopodiaceae, and *Ephedra*, while there are also Gramineae such as the *Poa annua*. The main shrub species distributed in the delta of Amu Darya River are *Suaeda physophora*, *Tamarix chinensis*, *Haloxylon ammodendron*, *Lycium ruthenicum*, *Halostachys capsica*, and *Calligonum mongolicum*, at a farther distance from the lakeside, the vegetation distribution consists of *Phragmites australis*, *Tamarix passerinoides*, *Halostachys capsica*, and *Suaeda physophora*. The alluvial meadow of the Tugayi forest at the front of the Syr River delta decreased, and the *Phragmites australis* was sparse with soil drought. The formerly dense undergrowth of the central delta, such as *Elaeagnus pungens*, *Salix babylonica*, *Halimodendron halodendron*, and *Tamarix passerinoides*, has become very sparse, and the *Calamagrostis epigeios* and *Phragmites australis* have disappeared, replaced by *Alhagi sparsifolia*, and *Salsola collina* (Table 1).

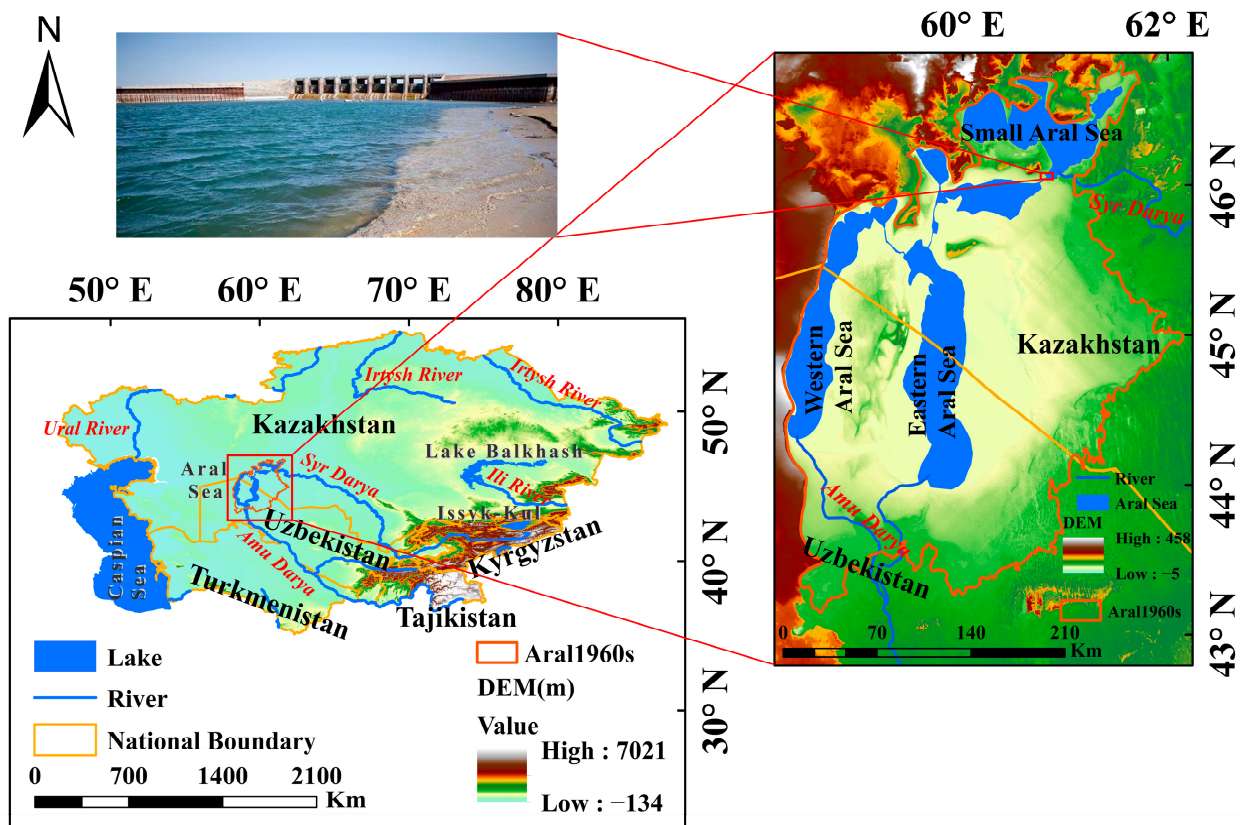


Figure 1. Location of the Aral Sea.

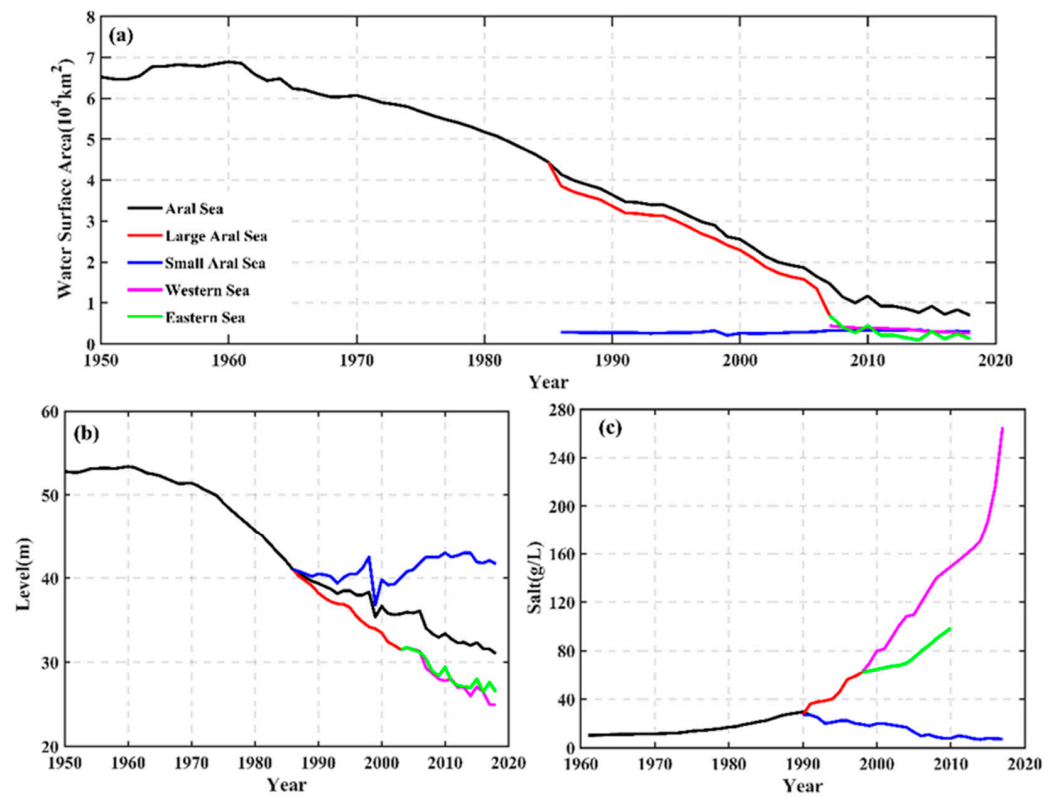


Figure 2. Changes in water level and area of the Aral Sea since the 1950s: (a) water surface area; (b) level; (c) salt. Source: [67].

Table 1. List of lake ecosystem vegetation survey 2019 in Large Aral Sea.

Latin Names	Families
<i>Phragmites australis</i> (Cav.) Trin. ex Steud.	Gramineae
<i>Haloxylon ammodendron</i> (C. A. Mey.) Bunge.	Chenopodiaceae
<i>Tamarix chinensis</i> Lour.	Tamaricaceae
<i>Calamagrostis epigeios</i> (L.) Roth.	Gramineae
<i>Seriphidium santolinum</i> (Schrenk) Poljak.	Compositae
<i>Alhagi sparsifolia</i> Shap.	Leguminosae
<i>Halostachys caspica</i> C. A. Mey. ex Schrenk.	Chenopodiaceae
<i>Halimodendron halodendron</i> (Pall.) Voss.	Leguminosae
<i>Lycium ruthenicum</i> Murray.	Solanaceae
<i>Suaeda physophora</i> Pall.	Chenopodiaceae
<i>Calligonum caput-medusae</i> Schrenk.	Polygonaceae
<i>Salsola collina</i> Pall.	Chenopodiaceae

2.2. Data Sources

The Landsat products were downloaded from the United States Geological Survey (USGS) online web portal. The scenes in 1987, 1997, 1992, 2007, and 2010 were first-level spectral data products from Landsat4 and Landsat5 Thematic Mapper (TM), with a spatial resolution of 30 m and a temporal resolution of 16 d. The scenes in 2014, 2015, 2017, and 2018 were first-level multispectral data products from Landsat8 OLI (Operational Land Imager) and TIRS (Thermal Infrared Sensor) with a spatial resolution of 30 m and a temporal resolution of 16d (Table 2).

Table 2. Remote sensing data sources. Source: [68].

Data Sources	Time	Path/Row	Spatial Resolution (m)	Temporal Resolution (d)
Landsat 5 TM	1987	p160/r28-30	30	16
	1992	p161/r27-30		
	1997	p162/r28-30		
	2007			
	2010			
Landsat 8 OLI	2014	p160/r28-30	30	16
	2015	p161/r27-30		
	2017	p162/r28-30		
	2018			

ENVI5.3 and ArcGIS10.2.2 were used for radiometric calibration and band fusion of the original remote sensing image. According to the shoreline of the Aral Sea in different years, the scope of the lakeside was determined and formed the contours of the study area in different periods (Figure 3). The NDVI tool in ENVI 5.3 Toolbox was used to calculate the band of images and the NDVI value from May to October was obtained. A maximum value composite (MVC) method was applied to obtain the annual NDVI data by reducing the atmospheric effects of clouds and aerosols [69,70]. The average NDVI for the growing season, spring, summer, and autumn was calculated for analysis. Pixels location with NDVI values of a month in the growing season not greater than zero were also masked and excluded from the study to decrease the effects of snow cover and water.

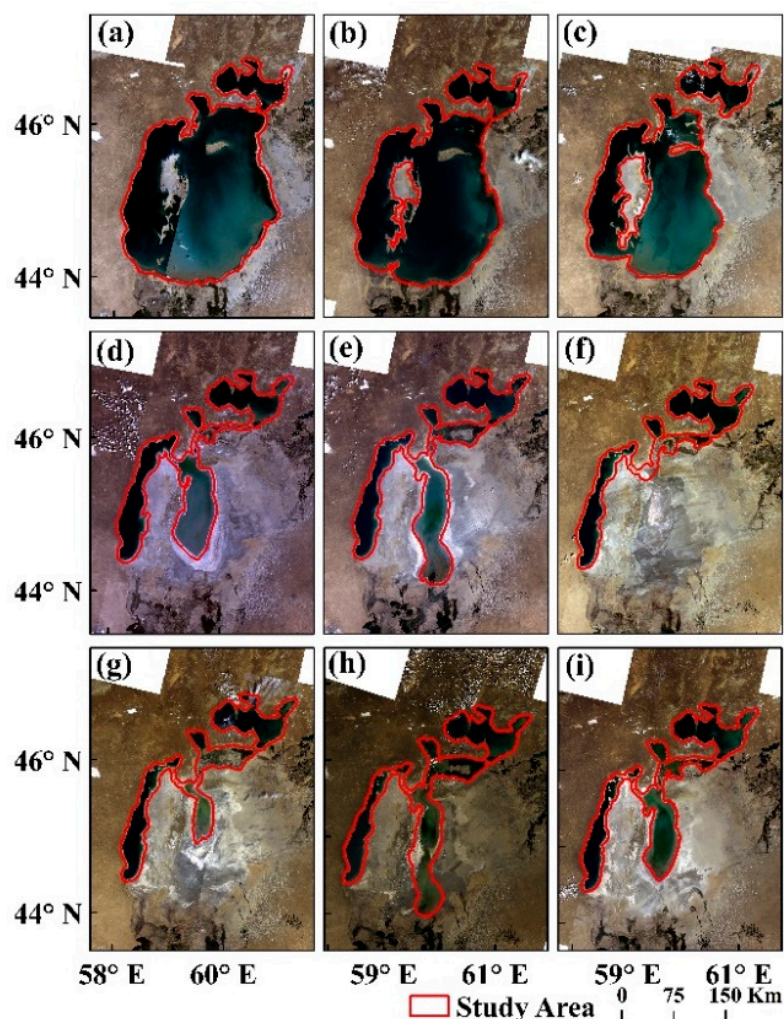


Figure 3. Remote sensing images and contours of the Aral Sea: (a) 1987; (b) 1992; (c) 1997; (d) 2007; (e) 2010; (f) 2014; (g) 2015; (h) 2017, and (i) 2018.

Data on the Aral Sea's water surface area and water level were obtained from the Portal of Knowledge for Water and Environmental Issues in Central Asia. The meteorological data are based on the time series (TS) high resolution ($0.5 \times 0.5^\circ$) monthly variation grid data provided by the Grid Climatic Research Unit (CRU) of the University of East Anglia. The data version is 4.04. The temperature and precipitation data from 1960 to 2018 are used.

2.3. Analysis Methods

2.3.1. Normalized Difference Vegetation Index (NDVI) and Maximum Value Composite (MVC)

The Normalized Difference Vegetation Index (NDVI) shows light absorbance and reflectance. For each pixel, we then calculated the NDVI using the following equation [22]:

$$NDVI = (NIR - Red) / (NIR + Red) \quad (1)$$

where *NIR* represents the reflectance in the near-infrared region of the electromagnetic spectrum and *Red* represents the reflectance in the red region of the electromagnetic spectrum.

To study the overall changes in vegetation in space, monthly NDVI and annual NDVI values were obtained by the Maximum Value Composite (MVC), which can effectively

reduce the influence of atmospheric aerosols, cloud shadows, solar altitude angles, and other factors [71]. The formula is as follows:

$$MaxNDVI_i = Max(NDVI_1, NDVI_2, NDVI_3, NDVI_4) \quad (2)$$

where $MaxNDVI_i$ indicates the maximum monthly $NDVI$; i indicates the month, and the value ranges from 5 to 10. $NDVI_1-NDVI_4$ represent the preprocessed $NDVI$ values of the original images in corresponding months.

2.3.2. Buffer Analysis

Buffer analysis is a common spatial geometric relationship analysis tool in ArcGIS for analyzing spatial proximity. The buffer zone is a band-shaped buffer area with a specific distance established around the spatial objects of different geometric types to represent the specific influence range or service range of the spatial target. It is used to analyze the influence of the geographical object on the surrounding spatial elements [72,73]. From the perspective of GIS technology, the buffer zone refers to a buffer polygon area with a specified width generated by setting a buffer radius of a specific value around geographic elements such as points, lines, and areas. Because of the different geometries of spatial objects, the construction mode of the buffer is also different. From a mathematical point of view, a buffer is a set of spaces that meet certain conditions, and the mathematical expression is:

$$B_i = (x : d(x, O_i) \leq R) \quad (3)$$

where O_i is the object, R is the neighborhood radius, d is the minimum Euclidean distance, and B_i is a set of all points whose distance from O_i is less than or equal to R .

As an independent data layer for overlay analysis, the buffer zone can be applied to spatial analysis such as roads, rivers, and residential areas [74]. Hu et al. [10] determined that the width of the Lake Taihu buffer zone is 2 km based on literature research, domestic and foreign river lake buffer zone research, and field investigations. In this study, the buffer zone of the Aral Sea is initially set as 3 km, and 3 km away from the present lake shoreline is taken as the research area. The use of buffer area analysis to establish the Aral Sea as the center of the circle, the search distance is 3 km, and the interval is 0.25 km.

2.3.3. Trend Analysis

We used linear regression to analyze the variation and intensity of $NDVI$ in the growing season of vegetation [73]. The regression analysis was used to analyze the change in the maximum $NDVI$ in the buffer zone from 1987 to 2018. The trend of $NDVI$ in each grid of remote sensing images from 1987 to 2018 was fitted pixel by pixel to obtain the trend of $NDVI$ in the study period, and the linear regression relationship between variable $NDVI_i$ and time t was established. The slope represents the rate of change of variable x_i . When $slope > 0$, this means that the growing season $NDVI$ is increasing during the study period. When $slope = 0$, it indicates that this variable does not change [75,76]. The greater the absolute value of $slope$, the greater the change in variable x_i .

$$slope = \frac{n \sum_{i=1}^n NDVI_i t_i - \sum_{i=1}^n NDVI_i \sum_{i=1}^n t_i}{n \sum_{i=1}^n t_i^2 - (\sum_{i=1}^n t_i)^2} \quad (4)$$

where n is the number of years in the monitoring period ($n = 9$); $NDVI_i$ is the maximum value of $NDVI$ in the growing season of different years.

2.3.4. Correlation Analysis between Vegetation Dynamics and Lake Hydrology

NDVI can be fitted by Unitary Linear Regression (ULR) analysis in this study to represent the influence of lake hydrology, including the area and the level of the lake. Correlation coefficients were used [77]:

$$r_{xy} = \frac{\sum_{i=1}^n (x_i - \bar{x})(y_i - \bar{y})}{\sqrt{\sum_{i=1}^n (x_i - \bar{x})^2} \sqrt{\sum_{i=1}^n (y_i - \bar{y})^2}} \quad (5)$$

where \bar{x} and \bar{y} represent the average values of the sample values of the two elements; r_{xy} is the correlation coefficient between x and y , indicating the correlation between the two elements with a value between $[-1, 1]$.

3. Results

3.1. Temporal Variation Trends of $NDVI_{max}$

3.1.1. Temporal Variation in the Aral Sea

The area-weighted average of the $NDVI_{max}$ of the Aral Sea buffer zone during the growing season from 1987 to 2018 ranges from 0.09 to 0.19, and the trend is $-0.173 \times 10^{-2} \text{ a}^{-1}$ ($p < 0.005$)—a fluctuating downward trend over time (Figure 4a). NDVI had a downward trend from 1987 to 1992, a slow rise from 1992 to 2007, and a decline again from 2007 to 2017. NDVI reached its lowest point in 2017, and slightly increased in 2018.

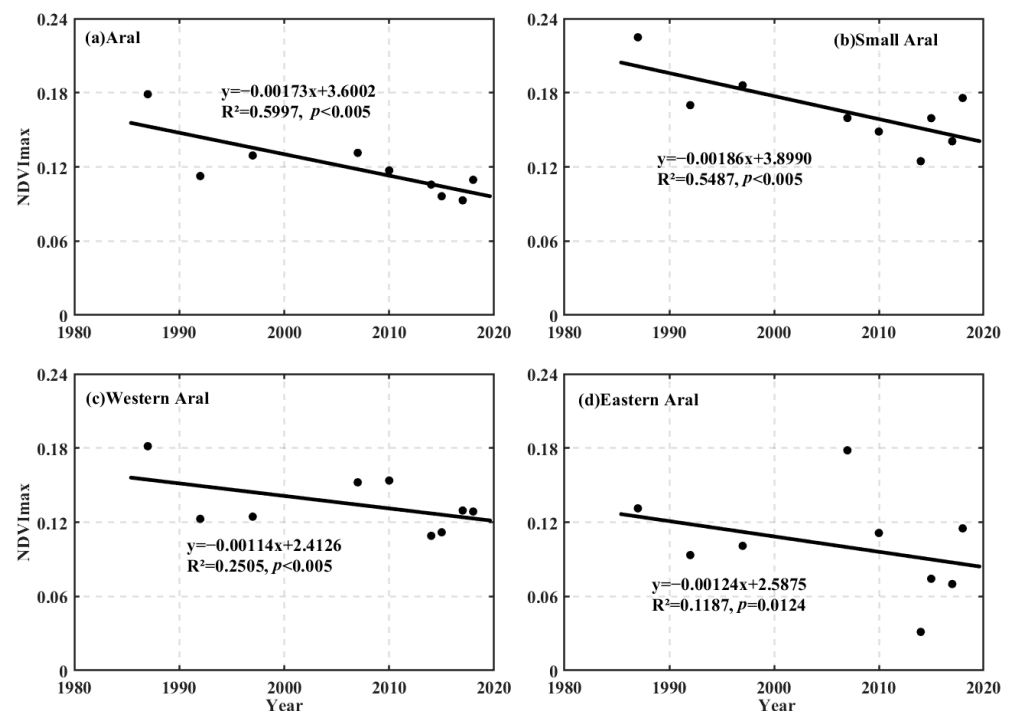


Figure 4. Changes in $NDVI_{max}$ during growing season in the study area from 1987 to 2018. (a): temporal variation of $NDVI_{max}$ in the Aral Sea; (b): temporal variation of $NDVI_{max}$ in the Small Aral Sea; (c): temporal variation of $NDVI_{max}$ in the west bank of the Western Aral; (d): temporal variation of $NDVI_{max}$ in the east bank of the Western Aral.

3.1.2. Temporal Variation in the Small Aral Sea

From 1987 to 2018, the area-weighted average of the $NDVI_{max}$ of the growing season in the buffer zone of the Small Aral Sea decreased over time (Figure 4b), ranged from 0.12–0.25, and the trend was $-0.186 \times 10^{-2} \text{ a}^{-1}$ ($p < 0.005$); from 1987 to 2014, the area-weighted average of the $NDVI_{max}$ decreased, and the trend was $0.29 \times 10^{-2} \text{ a}^{-1}$ ($p < 0.005$); from

2015 to 2018, the $NDVI_{max}$ during the growing season increased with the trend $0.84 \times 10^{-2} a^{-1}$ ($p = 0.003$).

3.1.3. Temporal Variation in the West Bank of the Western Aral

The area-weighted average of the $NDVI_{max}$ of the growing season in the buffer zone of the west bank of the Western Aral from 1987 to 2018 ranged from 0.10–0.19 and decreased over time (Figure 4c). The trend was $-0.114 \times 10^{-2} a^{-1}$ ($p < 0.005$). NDVI decreased from 1987 to 1997, increased from 1997 to 2010, and decreased again from 2010 to 2014. NDVI reached its lowest point in 2014 and slightly increased from 2014 to 2018.

3.1.4. Temporal Variation in the East Bank of the Eastern Aral

The area-weighted average of the $NDVI_{max}$ of the growing season in the buffer zone of the east bank of the Eastern Aral from 1987 to 2018 ranged from 0.03–0.18 and decreased over time (Figure 4d). The trend was $-0.124 \times 10^{-2} a^{-1}$ ($p < 0.005$). NDVI decreased from 1987 to 1997, increased from 1997 to 2010, and decreased again from 2010 to 2015. NDVI reached its lowest point in 2015 and slightly increased from 2015 to 2018.

3.2. Spatial Variation of Annual $NDVI_{max}$

3.2.1. Spatial Variation in the Aral Sea

From 1987 to 2018, the annual $NDVI_{max}$ in the growing season of the Aral Sea decreased with increasing distance from the lake within the 3 km buffer zone (Figure 5a). In other years, it is relatively stable, showing a downward trend within 0.25–1.25 km from the lake surface, and almost no change after 1.25 km. During the study period, the variation in annual $NDVI_{max}$ in the growing season of the 3 km buffer zone ranged from 0.09 to 0.2, with the minimum and maximum values appearing in 2017 and 1987, respectively. This indicates that within a range of 3 km lakeside, the $NDVI_{max}$ decreased with the distance from the lake; it tended to be stable after 1.25 km.

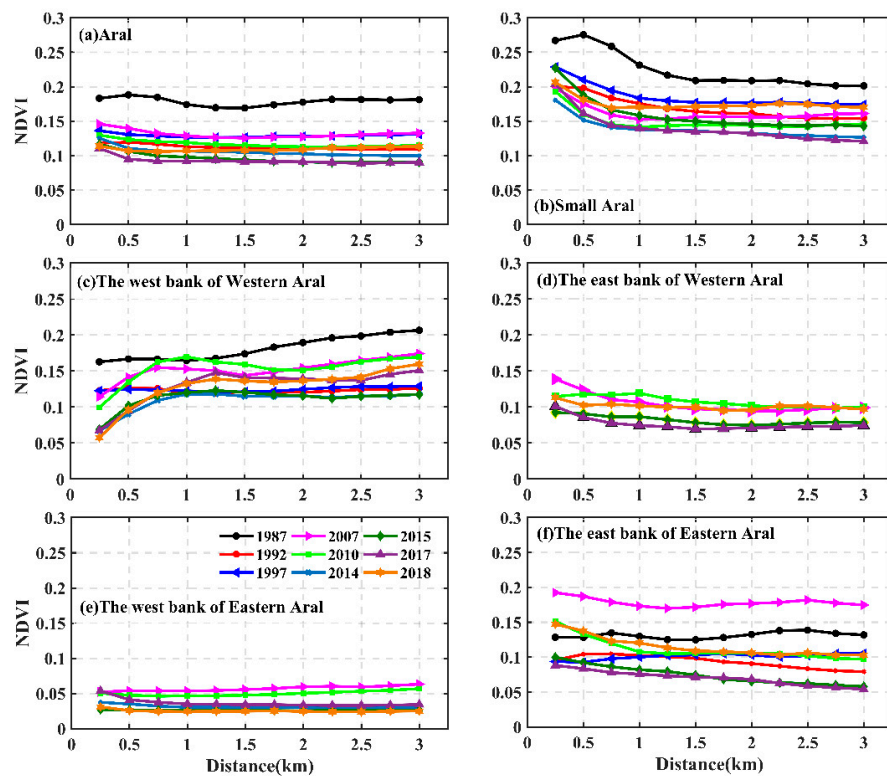


Figure 5. Variation of $NDVI_{max}$ in Aral Sea buffer zone from 1987 to 2018.

3.2.2. Spatial Variation in the Small Aral Sea

The annual $NDVI_{max}$ the growing season of the Small Aral Sea 1987–2018 decreased with increasing distance from the lake within the 3 km buffer zone (Figure 5b), and the value ranged from 0.12 to 0.3. In 1987, the annual $NDVI_{max}$ in the buffer zone fluctuated slightly within the study area, decreasing first and then stabilizing. Within 0.25–0.75 km from the lake, the annual $NDVI_{max}$ barely changed, it declined beyond 0.75 km and leveled off at about 1.5 km. After the 1990s, the annual $NDVI_{max}$ becomes stable, and the variation is similar each year. The annual $NDVI_{max}$ decreases within 1.0 km from the lake surface, and there is almost no change after 1.25 km, i.e., the buffer distance at which the annual $NDVI_{max}$ becomes stable is 1.25 km.

3.2.3. Spatial Variation in the Western Aral Sea

From 1987 to 2018, the annual $NDVI_{max}$ in the growing season of the west bank of the Western Aral first increased with increasing distance from the lake to 3 km and then tended to be stable (Figure 5c), with a range of 0.05–0.2. In 1987, the annual $NDVI_{max}$ increased within 3 km from the lake surface, with no obvious regularity. This was because the lakeside retreat of the west bank of the Western Aral Sea was small from 1987 to 1997, and most of it was cliff within 3 km. In 2007 and 2010, the annual $NDVI_{max}$ increased within 1 km from the lake surface and then decreased. Farther than 1.75 km from the lake's surface, the annual $NDVI_{max}$ increased again. After 2010, it rapidly increased within 1.25 km from the lake surface and tended to be stable after 1.25 km, i.e., the buffer distance at which the annual $NDVI_{max}$ becomes stable is 1.25 km.

From 1987 to 2018, the annual $NDVI_{max}$ in the growing season of the east bank of the Western Aral Sea first decreased with increasing distance from the lake within 3 km and then tended to be stable (Figure 5d), with a range of 0.04–0.15 and the variation of each year similar. The annual $NDVI_{max}$ first decreased within 1.0 km from the lake. Farther than 1.25 km, there is almost no change, i.e., the buffer distance when the annual $NDVI_{max}$ reaches a stable value is 1.25 km. This indicates that the annual $NDVI_{max}$ after 1.25 km is little affected by lake water.

3.2.4. Spatial Variation in the Eastern Aral Sea

From 1987 to 2018, the annual $NDVI_{max}$ in the growing season of the west bank of the Eastern Aral barely changed within the range of 3 km (Figure 5e), and the value ranged from 0 to 0.1, indicating mostly bare land. The east bank of the Western Aral is a newly exposed lake basin after the retreat of the Aral Sea and the vegetation is not established. This indicates that the annual $NDVI_{max}$ is not affected by lake water.

From 1987 to 2018, the annual $NDVI_{max}$ in the growing season of the east bank of the Eastern Aral decreased slightly with increasing distance from the lake within 3 km of the lakeside and showed a steady trend with the range of 0.04–0.2 (Figure 5f). The annual $NDVI_{max}$ in 2007 was the largest, and the vegetation growth was better. In 1987, the annual $NDVI_{max}$ fluctuated with increasing distance, but the change was not large. The other years showed a decreasing trend, but the change was small.

3.3. Driving Forces of Vegetation Change

3.3.1. Driving Forces of Vegetation Change in the Aral Sea

The growth of vegetation is inseparable from water. The $NDVI_{max}$ in the study area has a significant positive correlation with the water level of the Aral Sea and the lake area (Figure 6a,b). With the increase in the water level of the Aral Sea and the increase in the lake area, the $NDVI_{max}$ of the vegetation increases significantly. Among them, the correlation with water level is more significant.

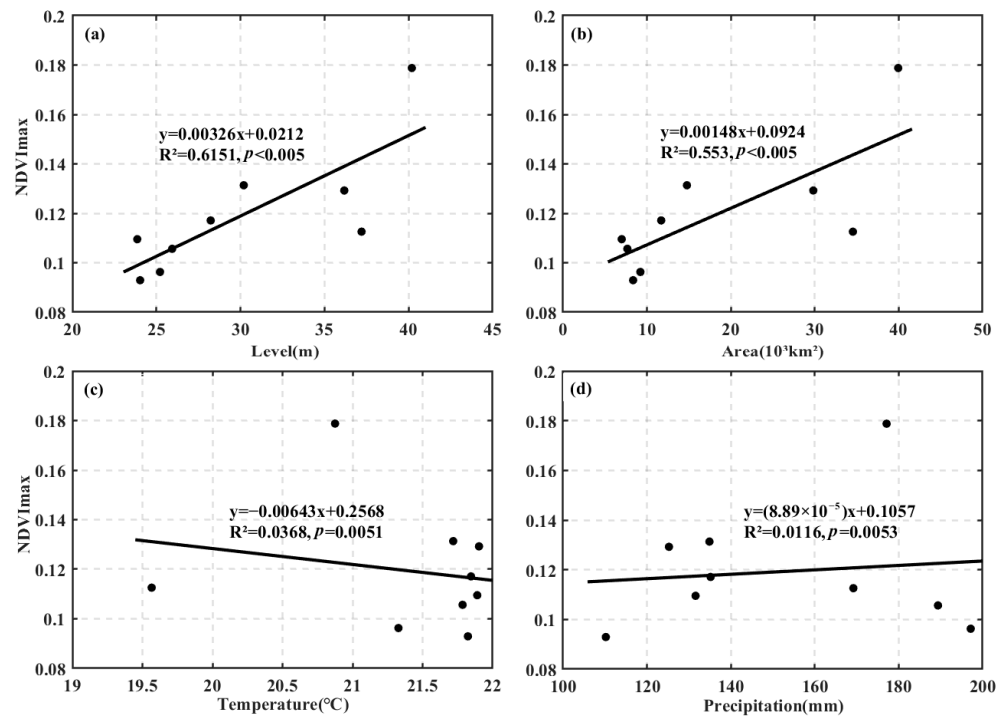


Figure 6. The relationship between $NDVI_{max}$ and driving factors in the study area from 1987 to 2018. (a): water level; (b): lake surface area; (c): temperature; (d): precipitation.

Since the 1960s, the annual precipitation in the Aral Sea research area changed slightly (Figure 7a), while the average temperature in the growing season increased (Figure 7b). There is no significant correlation between the $NDVI_{max}$ and the average temperature of the growing season and the annual precipitation in the study area. In particular, there is a weak negative correlation between $NDVI_{max}$ and the temperature (Figure 6c,d), which decreases with the increase in the average temperature of the growing season. There is no correlation with annual precipitation.

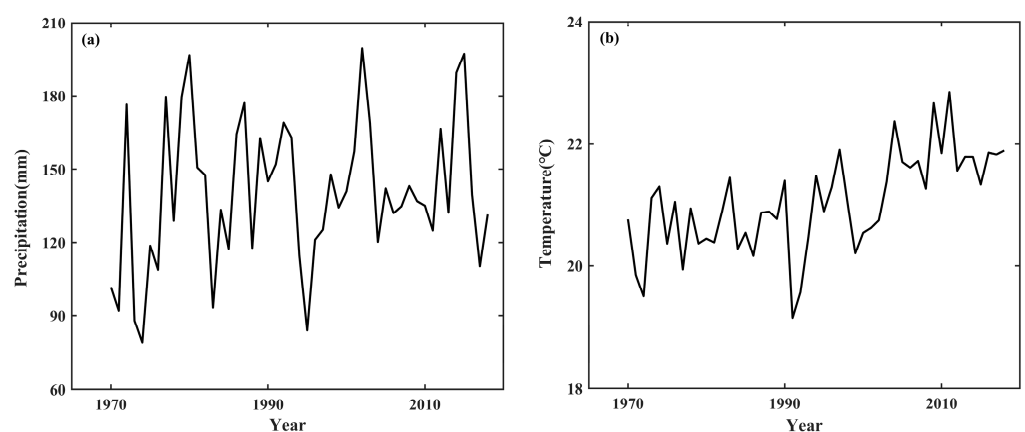


Figure 7. Variation of precipitation and growing season temperature in the Aral Sea during 1960–2018. (a): Precipitation; (b): growing season temperature.

3.3.2. Driving Forces of Vegetation Change in the Small Aral Sea and the West Bank of the Western Aral

As the Aral Sea recedes, the salt content of different parts varies. During the study period, the salt content of the Small Aral Sea changed little, with a maximum value of 26.35 g/L. The $NDVI_{max}$ was positively correlated with the salt content of the lake water

(Figure 8a), and the $NDVI_{max}$ increased with the increase in the salt content of the Aral Sea. The salt content of the Western Aral increased rapidly as the retreat intensified, with a maximum value of 265.455 g/L. The $NDVI_{max}$ in the study area on the west bank of the Western Aral showed a weak negative correlation with the salt content in the lake (Figure 8a) and the $NDVI_{max}$ decreased with the increase in salt content in the Western Aral.

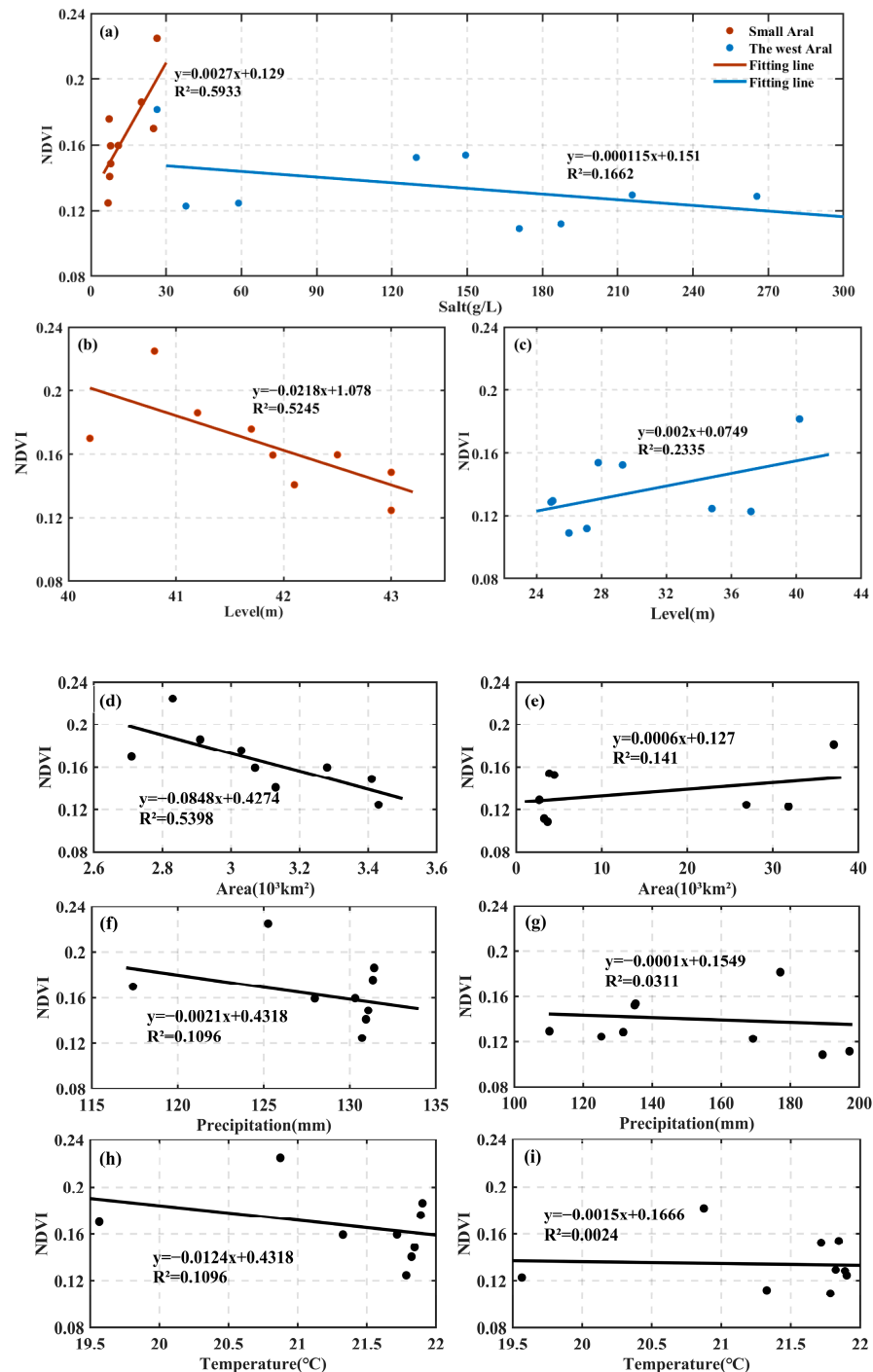


Figure 8. The relationship between $NDVI_{max}$ and driving factors in the study area from 1987 to 2018. (a): the salt of the Small Aral Sea and the Western Aral; (b): the level of the Small Aral Sea; (c): the level of the west bank of the Western Aral (d): the surface area of the Small Aral Sea; (e): the surface area of the west bank of the Western Aral (f): the precipitation of the Small Aral Sea; (g): the precipitation of the west bank of the Western Aral (h): the temperature of the Small Aral Sea (i): the temperature of the west bank of the Western Aral.

The lake area and water level of the Small Aral Sea did not change significantly during the study period and the $NDVI_{max}$ in the study area was not significantly correlated with the lake level (Figure 8b) but was negatively correlated with the lake area (Figure 8d). The lake area and water level of the Western Aral decreased rapidly, and $NDVI_{max}$ of the study area of the Western Aral showed a significant positive correlation with the lake level (Figure 8c) and a weak positive correlation with the lake area (Figure 8e).

There was no significant correlation between the $NDVI_{max}$ in the study area of the Small Aral Sea and the west bank of the Western Aral with the annual precipitation and the mean temperature of the growing season (Figure 8f–i).

4. Discussion

The vegetation changes in dry lake bed [46,78], lakeside wetland [79], and river delta are related to wetland changes [80] caused by lake changes. In nearly 60 years since 1960, the structure, function, and spatial pattern of the vegetation ecosystem have continuously evolved. Groundwater depth is an important driving force for the change in spatial and temporal patterns of ecosystems [81]. In arid desert environments, the water required by woody plants cannot be satisfied solely by natural precipitation, so vegetation formed by woody plants with stronger soil and water conservation function is strongly affected and controlled by groundwater depth, river, wetland, and lake distribution [82,83]. The retreat of the Aral Sea has been shown to affect the environment in some studies [36,37], and the loss of vegetation is one of them. Li et al. [23,24] use the NDVI time series to find the monotonic trend of vegetation, in the present study, the results showed that the area-weighted average of the $NDVI_{max}$ in the growing season of the Aral Sea was between 0.09 and 0.19, showing a decreasing trend. Whereas the vegetation along the lakeshore of the Small Aral Sea deteriorated after the sea is destroyed, the completion of the Kok-Aral Dam provided a better environment for its growth and development and the vegetation begins to recover [66]. Between 2005 and 2014, the water level fluctuated with drought and flood years; however, in general, the water level and area of the Small Aral Sea tended to be stable, providing a basis for the germination and growth of lakeside vegetation. The $NDVI_{max}$ in the lakeside growing season of the Small Aral Sea decreased before 2014 and increased after 2014. The completion of the Kok-Aral Dam was a death sentence for the Large Aral Sea. Water flowing from the Syr River into the desert basin only flows into the Small Aral Sea, and the Large Aral Sea has undergone drastic changes. The environment of the Large Aral Sea has undergone great changes with the retreat of the lake surface, and the vegetation was severely damaged. The vegetation growth of the different shores of the East and West Aral Sea varies, but the vegetation growth of the whole is relatively poor, especially the East Aral Sea with almost no vegetation growth and thus just a large area of bare land. The west bank of the Western Aral is a cliff, and with the retreat of the lake, the lake bed is exposed, which provides more space for the growth of vegetation. The water available to vegetation on the west coast also became a key factor affecting its growth and development, and the lake level showed a significant positive correlation with $NDVI_{max}$. Since 1987, the newly exposed lake basin on the west coast of the West Aral Sea is about 2 km, and the exposed lake basin provides space for the settlement of lakeside vegetation. The vegetation growth dynamics beyond 2 km were not analyzed. NDVI can reflect changes in vegetation coverage, but there is no characterization of the types of vegetation that grows or how the vegetation community changed.

Through field investigation, in the environmental deterioration of the Aral Sea, the soil of the lake bed exposed at different periods from the far shore to the lakeside showed obvious plant species gradients. We found there was obvious spatial heterogeneity in the growth of lakeside vegetation. Within a range of 3 km lakeside, the $NDVI_{max}$ decreased and was higher with the distance from the lake; it tended to be stable after 1.25 km. Within the lakeside buffer, with the increase in the distance from the lakeside, the lake provides less water for vegetation, and there is a difference in vegetation growth. Within 1.25 km

from the lakeside, the farther the distance from the lakeside, the soil and influence of the lake will be weaker on vegetation.

Yang et al. [40] found that human activities (especially irrigation and damming) are the dominant factors influencing the long-term variations of the Aral Sea. Similarly, Micklin [48] believed that irrigated water withdrawal was the dominant factor causing the recession of the Aral Sea from 1911 to 2010. Nik et al. [22] proved that more constant and moderate conditions at the riparian site benefited the growth and productivity of the common reed, we also found the annual in the lakeside area of the Aral Sea was significantly affected by the water level and lake surface area, showing a significant positive correlation. Therefore, the shrinkage of the Aral Sea caused by human factors is an important factor affecting the growth of Aral Sea vegetation.

Due to the decrease in the water level of the Aral Sea, the water is gradually concentrated and the water quality changes [84], the salt gradually increased and began to form a hard salt crust along the shore of the lake. With the further decrease in the water level, the salt crust gradually evolved into salty soil under a series of physical effects such as drying and weathering; under wind erosion, the salt soil further evolves into other types of bare land [34]. This is the biggest obstacle preventing ecological restoration and environmental improvement of the Aral Sea region. However, halophytes have strong salt tolerance. Halophytic vegetation has a certain resistance to salt concentration, and a certain concentration of salt can promote germination. Therefore, with the increase in salt in the Aral Sea, there is still some vegetation growth, and vegetation types have changed from shrubs to more salt-tolerant herbs. The salinity of the Small Aral Sea was stable (~ 30 g/L), which has little influence on the growth of halophytic vegetation. With natural succession, vegetation began to grow and settle, and $NDVI_{max}$ increased but showed a positive correlation with salt. Halophytic vegetation of the Large Aral Sea adapts to the harsh growth environment and begins to grow, but salt is still an important factor restricting its growth and development, and $NDVI_{max}$ is negatively correlated with salt. Within 2 km, the salt of the West Aral Sea increased with time. The closer the lake is to the shore, the higher the salt concentration is, which is more unfavorable to the growth of vegetation. On the contrary, with the increase in the distance from the lake shore, the soil salinity decreased and the halophytic vegetation could grow in the adapted environment. The $NDVI_{max}$ increased with increasing the distance from the lake shore at 1.25 km.

5. Conclusions

Based on buffer zone analysis and trend analysis, we analyzed trends of lakeside vegetation in the Aral Sea with the retreat of the lake and discussed the driving factors of the change in the Aral Sea vegetation. The results showed that the area-weighted average of the $NDVI_{max}$ in the growing season of the Aral Sea was between 0.09 and 0.19, showing a decreasing trend; the $NDVI_{max}$ in the lakeside growing season of the Small Aral Sea decreased before 2014 and increased after 2014; the $NDVI_{max}$ in the growing season for the East Aral Sea and West Aral Sea showed a fluctuating decline. There was obvious spatial heterogeneity in the growth of lakeside vegetation. Within a range of 3 km lakeside, the $NDVI_{max}$ decreased and was higher with the distance from the lake; it tended to be stable after 1.25 km.

The impact of human activities on the growth of vegetation in the buffer zone of the Aral Sea is crucial and overrides the impacts of climate change. The annual $NDVI_{max}$ in the lakeside area of the Aral Sea was significantly affected by the water level and lake surface area, showing a significant positive correlation. This had little to do with changes in temperature and precipitation. There was a positive correlation between the annual $NDVI_{max}$ and the salt content of the lake in the Small Aral Sea area. On the west bank of the Western Aral, the annual $NDVI_{max}$ was negatively correlated with the salt content of the lake, and significantly positively correlated with the lake level. The effects of annual precipitation and the average temperature of the growing season on the annual $NDVI_{max}$ in the study area of the Small Aral Sea and the west bank of the Western Aral were

not significant. Therefore, the shrinkage of the Aral Sea caused by human factors is an important factor affecting the growth of Aral Sea vegetation.

Author Contributions: Conceptualization, Y.W.; methodology, collected and processed the data, writing—original draft preparation, M.C.; supervision, review and editing X.Z. and Y.L. All authors have read and agreed to the published version of the manuscript.

Funding: This research was funded by the Strategic Priority Research Program of Chinese Academy of Sciences (no. XDA2006030102); and the “Western Light” program of the Chinese Academy of Sciences (2019-XBQNXZ-B-003).

Data Availability Statement: The data that support the findings of this study are available from the corresponding author upon reasonable request.

Acknowledgments: The authors also thank the anonymous reviewers for their helpful comments and suggestions.

Conflicts of Interest: The authors declare that they have no known competing financial interest or personal relationships that could have appeared to influence the work reported in this paper.

References

- Dornhofer, K.; Oppelt, N. Remote sensing for lake research and monitoring—Recent advances. *Ecol. Indic.* **2016**, *64*, 105–122. [[CrossRef](#)]
- Moss, B. Cogs in the endless machine: Lakes, climate change and nutrient cycles: A review. *Sci. Total Environ.* **2012**, *434*, 130–142. [[CrossRef](#)] [[PubMed](#)]
- Wang, S.M.; Dou, H.S. *Chinese Lakes*; Science Press: Beijing, China, 1998.
- Ma, R.H.; Yang, G.S.; Duan, H.T.; Jiang, J.H.; Wang, S.M.; Feng, X.Z.; Li, A.N.; Kong, F.X.; Xue, B.; Wu, J.L.; et al. China’s lakes at present: Number, area and spatial distribution. *Sci. China Earth Sci.* **2011**, *54*, 283–289. [[CrossRef](#)]
- Klein, I.; Dietz, A.J.; Gessner, U.; Galayeva, A.; Myrzakhetov, A.; Kuenzer, C. Evaluation of seasonal water body extents in Central Asia over the past 27 years derived from medium-resolution remote sensing data. *Int. J. Appl. Earth Obs. Geoinf.* **2014**, *26*, 335–349. [[CrossRef](#)]
- Begue, A.; Vintrou, E.; Ruelland, D.; Claden, M.; Dessay, N. Can a 25-year trend in Soudano-Sahelian vegetation dynamics be interpreted in terms of land use change? A remote sensing approach. *Glob. Environ. Change* **2011**, *21*, 413–420. [[CrossRef](#)]
- D’Arrigo, R.D.; Malmstrom, C.M.; Jacoby, G.C.; Los, S.O.; Bunker, D.E. Correlation between maximum latewood density of annual tree rings and NDVI based estimates of forest productivity. *Int. J. Remote Sens.* **2000**, *21*, 2329–2336. [[CrossRef](#)]
- Carlson, T.N.; Ripley, D.A. On the relation between NDVI, fractional vegetation cover, and leaf area index. *Remote Sens. Environ.* **1997**, *62*, 241–252. [[CrossRef](#)]
- Novillo, C.J.; Arrogante-Funes, P.; Romero-Calcerrada, R. Recent NDVI Trends in Mainland Spain: Land-Cover and Phytoclimatic-Type Implications. *ISPRS Int. J. Geo-Inf.* **2019**, *8*, 43. [[CrossRef](#)]
- Hu, X.Z.; Xu, Q.J.; Jiang, L.J.; Dong, S.Y.; Jin, D.Y. A preliminary study on demarcation limits of lake buffer zones: A case study of Lake Taihu. *J. Lake Sci.* **2011**, *23*, 719–724.
- Lloyd, A.; Law, B.; Goldingay, R. Bat activity on riparian zones and upper slopes in Australian timber production forests and the effectiveness of riparian buffers. *Biol. Conserv.* **2006**, *129*, 207–220. [[CrossRef](#)]
- Schoonover, J.E.; Williard, K.W.J.; Zaczek, J.J.; Mangun, J.C.; Carver, A.D. Nutrient Attenuation in Agricultural Surface Runoff by Riparian Buffer Zones in Southern Illinois, USA. *Agrofor. Syst.* **2005**, *64*, 169–180. [[CrossRef](#)]
- Gitelson, A.A. Wide dynamic range vegetation index for remote quantification of biophysical characteristics of vegetation. *J. Plant Physiol.* **2004**, *161*, 165–173. [[CrossRef](#)]
- Sun, R.; Liu, C.; Zhu, Q. Relationship Between the Fractional Vegetation Cover Change and Rainfall in the Yellow River Basin. *Acta Geogr. Sin.* **2001**, *56*, 667–672.
- Huete, A. Ecology Vegetation’s responses to climate variability. *Nature* **2016**, *531*, 181–182. [[CrossRef](#)]
- Yang, J.; Gong, P.; Fu, R.; Zhang, M.H.; Chen, J.M.; Liang, S.L.; Xu, B.; Shi, J.C.; Dickinson, R. The role of satellite remote sensing in climate change studies. *Nat. Clim. Change* **2013**, *3*, 875, Erratum in *Nat. Clim. Change* **2014**, *4*, 74–74. [[CrossRef](#)]
- Tucker, C.J.; Slayback, D.A.; Pinzon, J.E.; Los, S.O.; Myneni, R.B.; Taylor, M.G. Higher northern latitude normalized difference vegetation index and growing season trends from 1982 to 1999. *Int. J. Biometeorol.* **2001**, *45*, 184–190. [[CrossRef](#)]
- Zhu, X.; Liu, D. Improving forest aboveground biomass estimation using seasonal Landsat NDVI time-series. *ISPRS J. Photogramm. Remote Sens.* **2015**, *102*, 222–231. [[CrossRef](#)]
- Vicente-Serrano, S.M.; Camarero, J.J.; Olano, J.M.; Martín-Hernández, N.; Peña-Gallardo, M.; Tomás-Burguera, M.; Gazol, A.; Azorin-Molina, C.; Bhuyan, U.; Kenawy, A.E. Diverse relationships between forest growth and the Normalized Difference Vegetation Index at a global scale. *Remote Sens. Environ.* **2016**, *187*, 14–29. [[CrossRef](#)]

20. Chavez, R.O.; Clevers, J.G.P.W.; Decuyper, M.; De Bruin, S.; Herold, M. 50 years of water extraction in the Pampa del Tamarugal basin: Can *Prosopis tamarugo* trees survive in the hyper-arid Atacama Desert (Northern Chile)? *J. Arid. Environ.* **2016**, *124*, 292–303. [[CrossRef](#)]
21. Dong, X.; Peng, B.; Sieckenius, S.; Raman, R.; Leskovar, D.I. Leaf water potential of field crops estimated using NDVI in ground-based remote sensing—Opportunities to increase prediction precision. *PeerJ* **2021**, *9*, e12005. [[CrossRef](#)]
22. Ojdanič, N.; Zelnik, I.; Holcar, M.; Gaberščik, A.; Golob, A. Contrasting Dynamics of Littoral and Riparian Reed Stands within a Wetland Complex of Lake Cerknica. *Plants* **2023**, *12*, 1006. [[CrossRef](#)] [[PubMed](#)]
23. Li, Q.; Zhang, C. An Analysis of Monotonic Trend of Vegetation Cover in China Based on NDVI time series. *Bull. Soil Water Conserv.* **2014**, *13*, 1989–1996.
24. Meng, M.; Niu, Z.; Ma, C.; Tian, H.F.; Pei, J. Variation Trend of NDVI and Response to Climate Change in Tibetan Plateau. *Res. Soil Water Conserv.* **2018**, *25*, 7.
25. Pan, Z.; Huang, J.; Zhou, Q.; Wang, L.; Cheng, Y.; Zhang, H.; Blackburn, G.A.; Yan, J.; Liu, J. Mapping crop phenology using NDVI time-series derived from HJ-1 A/B data. *Int. J. Appl. Earth Obs. Geoinf.* **2015**, *34*, 188–197. [[CrossRef](#)]
26. Toth, V.R. Monitoring Spatial Variability and Temporal Dynamics of Phragmites Using Unmanned Aerial Vehicles. *Front. Plant Sci.* **2018**, *9*, 728. [[CrossRef](#)]
27. Badr, G.; Hoogenboom, G.; Davenport, J.; Smithyman, J. Estimating growing season length using vegetation indices based on remote sensing: A case study for vineyards in Washington state. *Trans. Asabe* **2015**, *58*, 551–564.
28. Liu, J.Z.; Chen, Y.N. Analysis on Converse Succession of Plant Communities at the Lower Reaches of Tarim River. *Arid Land Geogr.* **2002**, *25*, 231–236.
29. Chen, H.Y.; Chen, Y.N. Changes of desert riparian vegetation along the main stream of Tarim River, Xinjiang. *Chin. J. Ecol.* **2015**, *34*, 3166–3173.
30. Chen, Y.N. *Study on Ecohydrological Problems of Tarim River Basin in Xinjiang*, 1st ed.; Science Press: Beijing, China, 2010; p. 28.
31. Satge, F.; Espinoza, R.; Zola, R.P.; Roig, H.; Timouk, F.; Molina, J.; Garnier, J.; Calmant, S.; Seyler, F.; Bonnet, M.P. Role of Climate Variability and Human Activity on Poopo Lake Droughts between 1990 and 2015 Assessed Using Remote Sensing Data. *Remote Sens.* **2017**, *9*, 218. [[CrossRef](#)]
32. Luo, J.H.; Li, X.C.; Ma, R.H.; Li, F.; Duan, H.T.; Hu, W.P.; Qin, B.Q.; Huang, W.J. Applying remote sensing techniques to monitoring seasonal and interannual changes of aquatic vegetation in Taihu Lake, China. *Ecol. Indic.* **2016**, *60*, 503–513. [[CrossRef](#)]
33. Zhang, Z.X.; Chang, J.; Xu, C.Y.; Zhou, Y.; Wu, Y.H.; Chen, X.; Jiang, S.S.; Duan, Z. The response of lake area and vegetation cover variations to climate change over the Qinghai-Tibetan Plateau during the past 30 years. *Sci. Total Environ.* **2018**, *635*, 443–451. [[CrossRef](#)]
34. Izhitkiy, A.S.; Zavialov, P.O.; Sapozhnikov, P.V.; Kirillin, G.B.; Grossart, H.P.; Kalinina, O.Y.; Zalota, A.K.; Goncharenko, I.V.; Kurbaniyazov, A.K. Present state of the Aral Sea: Diverging physical and biological characteristics of the residual basins. *Sci. Rep.* **2016**, *6*, 23906. [[CrossRef](#)]
35. Micklin, P.P. Desiccation of The Aral Sea—A Water Management Disaster in the Soviet-Union. *Science* **1988**, *241*, 1170–1175. [[CrossRef](#)]
36. Chen, Y.N.; Li, Z.; Fang, G.H.; Li, W.H. Large Hydrological Processes Changes in the Transboundary Rivers of Central Asia. *J. Geophys. Res. Atmos.* **2018**, *123*, 5059–5069. [[CrossRef](#)]
37. Micklin, P. The future Aral Sea: Hope and despair. *Environ. Earth Sci.* **2016**, *75*, 844. [[CrossRef](#)]
38. Perera, J. A Sea Turns to Dust. *New Sci.* **1993**, *140*, 24–27.
39. Micklin, P.P. The Aral Sea Problem. *Proc. Inst. Civ. Eng. Civ. Eng.* **1994**, *102*, 114–121.
40. Yang, X.W.; Wang, N.L.; Chen, A.A.; He, J.; Hua, T.; Qie, Y.F. Changes in area and water volume of the Aral Sea in the arid Central Asia over the period of 1960–2018 and their causes. *Catena* **2020**, *191*, 104566. [[CrossRef](#)]
41. Karami, S.; Hamzeh, N.H.; Kaskaoutis, D.G.; Rashki, A.; Alam, K.; Ranjbar, A. Numerical simulations of dust storms originated from dried lakes in central and southwest Asia: The case of Aral Sea and Sistan Basin. *Aeolian Res.* **2021**, *50*, 100679. [[CrossRef](#)]
42. Reimov, M.; Statov, V.; Reymov, P.; Mamutov, N.; Abdireymov, S.; Khudaybergenov, Y.; Matchanova, S.; Orazbaev, A. Evaluation of desertified delta plant communities using spectral indexes and landscape transformation models. *E3S Web Conf.* **2021**, *227*, 02006. [[CrossRef](#)]
43. Zhang, X.Y.; Liu, H.L.; Chen, H. Changes of vegetation and its forces driving in the Aral Sea Basin of Central Asia. *E3S Web Conf.* **2021**, *269*, 01013. [[CrossRef](#)]
44. Kochkarova, S.; Mambetullaeva, S. Study of Successional Processes of Vegetation Cover on the Dried Seabed of the Aral Sea. *J. Res. Lepid.* **2020**, *51*, 764–768. [[CrossRef](#)]
45. Wada, Y.; Reager, J.T.; Chao, B.F.; Wang, J.; Lo, M.-H.; Song, C.; Li, Y.; Gardner, A.S. Recent changes in land water storage and its contribution to sea level variations. *Surv. Geophys.* **2017**, *38*, 131–152. [[CrossRef](#)] [[PubMed](#)]
46. Kuz'mina, Z.V.; Treshkin, S. Formation of vegetation on solonchaks of the dried Aral Sea bed under changing climate conditions. *Russ. Agric. Sci.* **2009**, *35*, 37–41. [[CrossRef](#)]
47. Salehie, O.; bin Ismail, T.; Shahid, S.; Hamed, M.M.; Chinnasamy, P.; Wang, X.J. Assessment of Water Resources Availability in Amu Darya River Basin Using GRACE Data. *Water* **2022**, *14*, 533. [[CrossRef](#)]
48. Micklin, P. *Aral Sea Basin Water Resources and the Changing Aral Water Balance*; Springer: Berlin/Heidelberg, Germany, 2014.

49. Lioubimtseva, E.; Henebry, G.M. Climate and environmental change in arid Central Asia: Impacts, vulnerability, and adaptations. *J. Arid Environ.* **2009**, *73*, 963–977. [[CrossRef](#)]
50. Nezlin, N.P.; Kostianoy, A.G.; Lebedev, S.A. Interannual variations of the discharge of Amu Darya and Syr Darya estimated from global atmospheric precipitation. *J. Mar. Syst.* **2004**, *47*, 67–75. [[CrossRef](#)]
51. Pan, X.H.; Wang, W.S.; Liu, T.; Huang, Y.; De Maeyer, P.; Guo, C.Y.; Ling, Y.N.; Akmalov, S. Quantitative Detection and Attribution of Groundwater Level Variations in the Amu Darya Delta. *Water* **2020**, *12*, 2869. [[CrossRef](#)]
52. Gafforov, K.S.; Bao, A.; Rakhimov, S.; Liu, T.; Abdullaev, F.; Jiang, L.; Durdiev, K.; Duulatov, E.; Rakhimova, M.; Mukanov, Y. The Assessment of Climate Change on Rainfall-Runoff Erosivity in the Chirchik–Akhangan Basin, Uzbekistan. *Sustainability* **2020**, *12*, 3369. [[CrossRef](#)]
53. Ma, L.; Abuduwaili, J.; Li, Y.M.; Uulu, S.A.; Mu, S.Y. Hydrochemical Characteristics and Water Quality Assessment for the Upper Reaches of Syr Darya River in Aral Sea Basin, Central Asia. *Water* **2019**, *11*, 1893. [[CrossRef](#)]
54. Micklin, P.; Asian, C.; Prospects, C. *Managing Water in Central Asia*; Chatham House: London, UK, 2000; p. 28.
55. Sorrel, P.; Popescu, S.M.; Klotz, K.; Suc, J.P.; Oberhnsli, H. Climate variability in the Aral Sea basin (Central Asia) during the late Holocene based on vegetation changes-ScienceDirect. *Quat. Res.* **2007**, *67*, 357–370. [[CrossRef](#)]
56. Boomer, I.; Aladin, N.; Plotnikov, I.; Whatley, R. The palaeolimnology of the Aral Sea: A review. *Quat. Sci. Rev.* **2000**, *19*, 1259–1278. [[CrossRef](#)]
57. Nezlin, N.P.; Kostianoy, A.G.; Li, B.L. Inter-annual variability and interaction of remote-sensed vegetation index and atmospheric precipitation in the Aral Sea region. *J. Arid Environ.* **2005**, *62*, 677–700. [[CrossRef](#)]
58. Ayzel, G.; Izhitskiy, A. Climate Change Impact Assessment on Freshwater Inflow into the Small Aral Sea. *Water* **2019**, *11*, 2377. [[CrossRef](#)]
59. Low, F.; Navratil, P.; Kotte, K.; Scholer, H.F.; Bubenzer, O. Remote-sensing-based analysis of landscape change in the desiccated seabed of the Aral Sea—a potential tool for assessing the hazard degree of dust and salt storms. *Environ. Monit. Assess* **2013**, *185*, 8303–8319. [[CrossRef](#)]
60. Micklin, P.; Aladin, N.V. Reclaiming the aral sea. *Sci. Am.* **2008**, *298*, 64–71. [[CrossRef](#)]
61. Saiko, T.A.; Zonn, I.S. Irrigation expansion and dynamics of desertification in the Circum-Aral region of Central Asia. *Appl. Geogr.* **2000**, *20*, 349–367. [[CrossRef](#)]
62. Kezer, K.; Matsuyama, H. Decrease of river runoff in the Lake Balkhash basin in Central Asia. *Hydrol. Process.* **2006**, *20*, 1407–1423. [[CrossRef](#)]
63. Karthe, D.; Abdullaev, I.; Boldgiv, B.; Borchardt, D.; Chalov, S.; Jarsjo, J.; Li, L.H.; Nittrouer, J.A. Water in Central Asia: An integrated assessment for science-based management. *Environ. Earth Sci.* **2017**, *76*, 690. [[CrossRef](#)]
64. Duan, Z.H.; Wang, X.L.; Sun, L. Monitoring and Mapping of Soil Salinity on the Exposed Seabed of the Aral Sea, Central Asia. *Water* **2022**, *14*, 1438. [[CrossRef](#)]
65. Christopher, P. Ecological restoration. In Northern Aral Sea, rebound comes with a big catch. *Science* **2011**, *334*, 303.
66. Sharma, A.; Huang, H.P.; Zavialov, P.; Khan, V. Impact of Desiccation of Aral Sea on the Regional Climate of Central Asia Using WRF Model. *Pure Appl. Geophys.* **2018**, *175*, 465–478. [[CrossRef](#)]
67. Portal of Knowledge for Water and Environmental Issues in Central Asia. Regional Information System on Water and Land Resources in the Aral Sea Basin (CAWater-IS) Database. Available online: http://www.cawater-info.net/bd/index_e.htm (accessed on 13 May 2021).
68. United States Geological Survey (USGS). Landsat Database. Available online: <https://earthexplorer.usgs.gov/> (accessed on 6 August 2020).
69. Li, H.D.; Li, Y.K.; Gao, Y.Y.; Zou, C.X.; Yan, S.G.; Gao, J.X. Human Impact on Vegetation Dynamics around Lhasa, Southern Tibetan Plateau, China. *Sustainability* **2016**, *8*, 1146. [[CrossRef](#)]
70. Li, J.; Fan, K.; Zhou, L.M. Satellite Observations of El Nino Impacts on Eurasian Spring Vegetation Greenness during the Period 1982–2015. *Remote Sens.* **2017**, *9*, 628. [[CrossRef](#)]
71. Holben, B.N. Characteristics of maximum-value composite images from temporal AVHRR data. *Int. J. Remote Sens.* **1986**, *7*, 1417–1434. [[CrossRef](#)]
72. Duan, J.F.; Guo, Q.X.; Xie, H.Z. Research of Management System of Ecological Water Requirement of Vegetation Based on the GIS in Shanxi Yongding River. *Res. Soil Water Conserv.* **2011**, *18*, 5.
73. Zhang, H.B. Application of buffer analysis function of GIS in field plot management. *Mod. Agric.* **2015**, *426*, 61–62.
74. Xue, Y.; Brown, D.E. Spatial analysis with preference specification of latent decision makers for criminal event prediction. *Decis. Support Syst.* **2006**, *41*, 560–573. [[CrossRef](#)]
75. Luo, M.; Guli, J.; Guo, H.; Guo, H.; Liu, T. Spatial-temporal Variation of Growing-season NDVI and Its Responses to Hydrothermal Condition in the Tarim River Basin from 2000 to 2013. *J. Nat. Resour.* **2017**, *32*, 50–63.
76. Ye, Z.J.; OuYang, C.X.; Feng, Z.Y.; Fang, B. Analysis of the Dominance and Sustainability of Vegetation Cover in Lushan Nature Reserve. *Environ. Sustain. Dev.* **2015**, *40*, 5.
77. He, Y.; Fan, G.F.; Zhang, X.W.; Liu, M.; Gao, D.W. Variation of vegetation NDVI and its response to climate change in Zhejiang Province. *Acta Ecol. Sin.* **2012**, *32*, 11.
78. Walter, W. Vegetation Dynamics on the Dry Sea Floor of the Aral Sea. In *Sustainable Land Use in Deserts*; Springer: Berlin/Heidelberg, Germany, 2002; pp. 52–68.

79. Dimeyeva, L.A. *Methods of Conservation and Restoration of Vegetation Cover on the Aral Sea Coast*; Springer: Berlin/Heidelberg, Germany, 2001.
80. Ferrari, M.R.; Miller, J.R.; Russell, G.L. Modeling the effect of wetlands, flooding, and irrigation on river flow: Application to the Aral Sea. *Water Resour. Res.* **1999**, *35*, 1869–1876. [[CrossRef](#)]
81. Fan, Y. Groundwater in the Earth's critical zone: Relevance to large-scale patterns and processes. *Water Resour. Res.* **2015**, *51*, 3052–3069. [[CrossRef](#)]
82. Lopez-Portillo, J.; Montana, C. Spatial distribution of *Prosopis glandulosa* var. *torreyana* in vegetation stripes of the southern Chihuahuan Desert. *Acta Oecolog. Int. J. Ecol.* **1999**, *20*, 197–208. [[CrossRef](#)]
83. Martinez, A.J.; Lopez-Portillo, J. Allometry of *Prosopis glandulosa* var. *torreyana* along a topographic gradient in the Chihuahuan desert. *J. Veg. Sci.* **2003**, *14*, 111–120. [[CrossRef](#)]
84. Benduhn, F.; Renard, P. A dynamic model of the Aral Sea water and salt balance. *J. Mar. Syst.* **2004**, *47*, 35–50. [[CrossRef](#)]

Disclaimer/Publisher's Note: The statements, opinions and data contained in all publications are solely those of the individual author(s) and contributor(s) and not of MDPI and/or the editor(s). MDPI and/or the editor(s) disclaim responsibility for any injury to people or property resulting from any ideas, methods, instructions or products referred to in the content.